

Ocular Pulse Amplitude Correlates With Ocular Rigidity at Native IOP Despite the Variability in Intraocular Pulse Volume With Each Heartbeat

John E. Markert¹, Daniel C. Turner², Jessica V. Jasien², Cyril N. A. Nyankerh², Brian C. Samuels¹, and J. Crawford Downs¹

¹ Department of Ophthalmology and Visual Sciences, School of Medicine, University of Alabama at Birmingham, Birmingham, AL, USA

² Vision Science Graduate Program, School of Optometry, University of Alabama at Birmingham, Birmingham, AL, USA

Correspondence: J. Crawford Downs, Professor of Ophthalmology and Visual Sciences, University of Alabama at Birmingham School of Medicine, 1670 University Blvd., VH 390A, Birmingham, AL 35294, USA. e-mail: cdowns@uab.edu

Received: November 11, 2021

Accepted: August 2, 2022

Published: September 8, 2022

Keywords: ocular pulse amplitude; ocular rigidity; ocular pulse volume; nonhuman primate

Citation: Markert JE, Turner DC, Jasien JV, Nyankerh CNA, Samuels BC, Downs JC. Ocular pulse amplitude correlates with ocular rigidity at native IOP despite the variability in intraocular pulse volume with each heartbeat. *Transl Vis Sci Technol.* 2022;11(9):6. <https://doi.org/10.1167/tvst.11.9.6>

Purpose: The purpose of this study was to assess ocular coat mechanical behavior using controlled ocular microvolumetric injections (MVI) of 15 μL of balanced salt solution (BSS) infused over 1 second into the anterior chamber (AC) via a syringe pump.

Methods: Intraocular pressure (IOP) was continuously recorded at 200 Hz with a validated implantable IOP telemetry system in 7 eyes of 7 male rhesus macaques (nonhuman primates [NHPs]) during 5 MVIs in a series at native (3 trials), 15 and 20 mm Hg baseline IOPs, repeated in 2 to 5 sessions at least 2 weeks apart. Ocular rigidity coefficients (K) and ocular pulse volume (PV) were calculated for each trial. Data were averaged across sessions within eyes; PV was analyzed with a three-level nested ANOVA, and parameter relationships were analyzed with Pearson Correlation and linear regression.

Results: After MVI at native baseline IOP of 10.4 ± 1.6 mm Hg, IOP increased by 9.1 ± 2.8 mm Hg (ΔIOP) at a 9.6 ± 2.7 mm Hg/s slope, ocular pulse amplitude (OPA) was 0.70 ± 0.13 mm Hg on average; the average K was $0.042 \pm 0.010 \mu\text{L}^{-1}$ and average PV was $1.16 \pm 0.43 \mu\text{L}$. PV varied significantly between trials, days, and eyes ($P \leq 0.05$). OPA was significantly correlated with K at native IOP: Pearson coefficients ranged from 0.71 to 0.83 ($P \leq 0.05$) and R^2 ranged from 0.50 to 0.69 ($P \leq 0.05$) during the first trial.

Conclusions: The MVI-driven ΔIOP and slope can be used to assess ocular coat mechanical behavior and measure ocular rigidity.

Translational Relevance: Importantly, OPA at native IOP is correlated with ocular rigidity despite the significant variability in PV between heartbeats.

Introduction

Vision loss in glaucoma is driven by retinal ganglion cell (RGC) damage, primarily occurring as the axons exit the eye at the optic nerve head (ONH).^{1–5} Intraocular pressure (IOP) has been shown to be a principle risk factor for glaucoma in clinical studies,^{6–11} although other contributing factors, such as ocular perfusion pressure or blood flow,^{10–14} immune reactivity,^{15–17} and cerebrospinal fluid pressure, have been implicated.^{18–21} Lowering IOP is the only proven clinical treatment for slowing the onset and progression

of glaucoma in studies of mean IOPs measured using snapshot devices, such as tonometers.^{22–24} However, IOP has been shown to be very dynamic over both short and long timescales,^{25–28} although the contribution of transient IOP fluctuations to the disease and how current glaucoma treatments affect IOP fluctuations remain unknown. A recent study identified the primary sources of transient IOP fluctuations as blink, saccade, and ocular pulse amplitude (OPA), and determined that transient IOP fluctuations comprise an average of 12% of the total IOP-related mechanical energy that the eye must absorb during waking hours.²⁸

The magnitude of transient IOP fluctuations are related to ocular coat stiffness, with larger transient IOP fluctuations occurring with even small increases in corneal stiffness,^{29,30} peripapillary scleral stiffness,³¹ and baseline IOP.³² The primary relation used to quantify ocular coat stiffness was developed by Jonas Friedenwald and expressed through the Friedenwald equation, which defines ocular coat stiffness as the coefficient of ocular rigidity, K , which relates the change in IOP (ΔIOP) with ocular volume change ΔV , where $IOP = IOP_0 e^{K\Delta V}$, showing that ocular rigidity increases linearly with IOP but nonlinearly with changes in volume and ocular coat stretch.³³ In addition, OPA is larger at higher IOPs,^{32,34} presumably due to the tight autoregulation of ocular blood flow, as long as IOP is within a physiologic range.^{35–38} Prior studies have shown that there is significant variability in ocular pulse volume (PV), the volume of blood injected into the eye with every heartbeat.^{34,39}

Anterior chamber (AC) manometry is the primary invasive method used to measure ocular rigidity intraoperatively.^{34,40} Using this method, Dastiridou and coworkers found that OPA and ocular rigidity were correlated in human patients at controlled IOPs of 15, 20, 25, 30, 35, 40, and 45 mm Hg, suggesting that increased larger transient IOP fluctuations, such as OPA, are associated with greater ocular rigidity.³⁴ Importantly, however, this study did not test eyes at native IOP, which is the standard condition under which clinical examinations are administered, so this result cannot necessarily be generalized across eyes that present at a range of native IOPs. Several studies have shown promise in calculating ocular rigidity using noninvasive methods in human eyes based primarily on estimating ocular volume change using imaging.⁴¹ Beaton and colleagues used optical coherence tomography (OCT) in continuous 2D B-scan mode to estimate choroidal volume change with the cardiac cycle.³⁹ Sayah and coworkers improved on this approach, which was used along with OPA as a noninvasive method to estimate ocular rigidity in patients, and they reported reasonably good agreement ($R^2 = 0.74$) with gold standard invasive ocular rigidity measurements.⁴¹ Beaton, Ma, and coworkers also used these techniques to investigate their association with transient IOP fluctuations, and reported significant correlations between noninvasive estimated ocular rigidity and OPA, although the relationship was not particularly strong, with R^2 values of 0.09 and 0.26, respectively.^{39,41,42} Although many studies have found relevant relationships between IOP fluctuations and various aspects of the ocular coat biomechanical response using invasive methods,^{29,31,43} noninvasive clinical measurement of ocular rigidity

without significant estimation error remains elusive.

We have developed and validated a wireless telemetry system to continuously measure IOP at 200 Hz with indwelling sensors in Rhesus macaques,^{26–28,44} in which experimental glaucoma can be induced that is similar to human disease.^{45,46} The purpose of this study was to assess ocular coat biomechanical behavior using controlled microvolumetric injections (MVI) of sterile balanced saline solution into the living eye at native IOP, in order to relate those invasive measures to variables that can be measured noninvasively at native IOP, as well as compare ocular rigidity coefficients in nonhuman primates (NHPs) to that from patients at controlled IOPs.

Methods

Animals

All experiments were conducted in accordance with the ARVO Statement for the Use of Animals in Ophthalmic and Vision Research, using procedures approved by the Institutional Animal Care and Use Committee of the University of Alabama at Birmingham. This study is a part of a larger study analyzing potential relationships between transient IOP fluctuations and glaucomatous onset and progression. Seven normal eyes from seven young adult male Rhesus macaques (aged 5.5–7.5 years old) were used in this study (Table 1). Axial length was calculated using an automated ocular ultrasound probe (Sonomed PacScan 300AP; Sonomed Escalon, Inc., Lake Success, NY).

IOP Telemetry and Transducer Calibration

IOP was continuously recorded wirelessly 200 times per second during each MVI session using a validated implantable telemetry system (Stellar series custom implant, TSE-Systems, Chesterfield, MO) in which the piezoelectric pressure transducer is implanted directly in AC (Figs. 1, 2). Implants were allowed to heal in at least 6 weeks prior to MVI. Immediately after each multi-trial MVI testing session, IOP transducers were calibrated from 5 to 30 mm Hg in 5 mm Hg steps against an in-line digital pressure gauge (Model XP2i, Crystal Engineering, San Luis Obispo, CA) using AC manometry to ensure accurate readings. The system compensates for changes in atmospheric pressure in real time, and all data were acquired with the NOTOCORD-hem data acquisition system (NOTOCORD Systems, Le Pecq, France)

Table 1. Animal Demographics

NHP	Eye	Age (yr)	Sex	No. of Sessions	Axial Length (mm)
13.171	OD	5.5	Male	3	19.56
13.86	OD	5.5	Male	3	19.19
150069	OD	6	Male	2	21.64
150110	OD	6	Male	5	19.82
150152	OD	7.5	Male	4	19.41
150152	OS	7.5	Male	4	19.55
150171	OD	7	Male	4	19.86
150171	OS	7	Male	4	19.89
150172	OS	7	Male	3	20.58

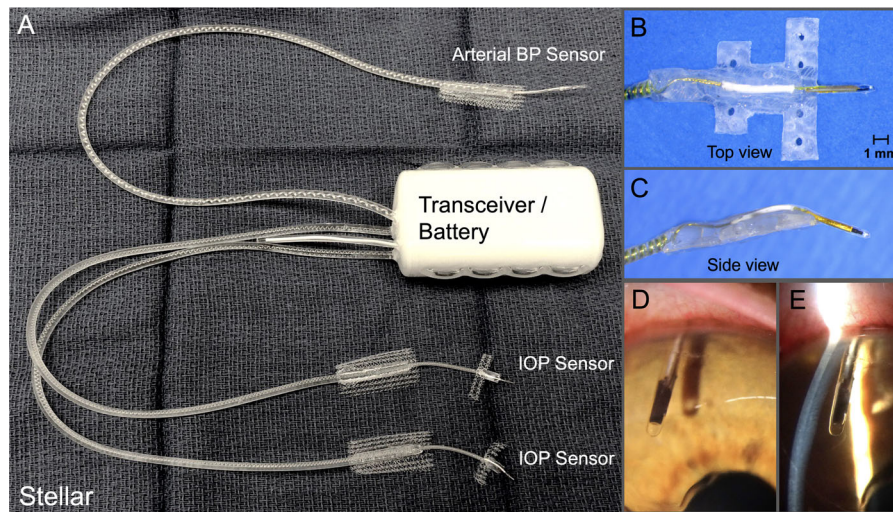


Figure 1. (A) TSE Stellar BP/IOP total implant system. (B) Top view of the IOP transducer and integrated scleral baseplate. (C) Side view of the IOP transducer and integrated scleral baseplate. (D) En face photograph of the piezoelectric IOP transducer in the anterior chamber. (E) Slit lamp photograph of the intraocular placement of the piezoelectric IOP transducer in the anterior chamber relative to the cornea and iris. Adapted from Jasien et al.,⁴⁷ with permission.

and analyzed after calibration offset corrections were applied with software postprocessing.

Microvolumetric Injections

For each MVI session, the NHP was anesthetized with an intramuscular injection of ketamine (3 mg/kg) and dexmedetomidine (0.05 mg/kg). The AC was cannulated with a 27-gauge needle inserted through the cornea at the limbus, which was connected to a manometer bottle of balanced salt solution (BSS) via a sterile infusion set fitted with an in-line digital pressure gauge level with the needle insertion into the eye. A constant-rate infusion of 15 μ L of sterile BSS over 1 second was introduced into each eye through a 3-way valve connecting the AC cannula to a programmable precision syringe pump (Model PhD, Harvard Apparatus,

Holliston, MA) fitted with 1 mL Hamilton Syringe (Hamilton Company, Reno, NV), as has been used in previous studies.^{29,31} This approach yields a 10 to 15 mm Hg elevation in IOP depending on the eye, with limited viscoelastic effects due to the short time scales,⁴⁸ and was chosen based on prior MVI studies in enucleated eyes.^{29–31} IOP was recorded continuously for 5 MVIs in each session in the following order: 3 MVIs at native IOP, one MVI at 15 mm Hg, and one MVI at 20 mm Hg. Note that native IOP is not significantly affected by anesthesia in NHPs, so this represents the natural resting IOP of an awake animal.⁴⁹ The manometer bottle was shut off entirely using the stopcock for the 3 MVIs at native IOP, raised to the 15 mm Hg reading on the in-line pressure gauge immediately prior to the fourth MVI, and raised to the 20 mm Hg reading on the in-line pressure gauge immediately

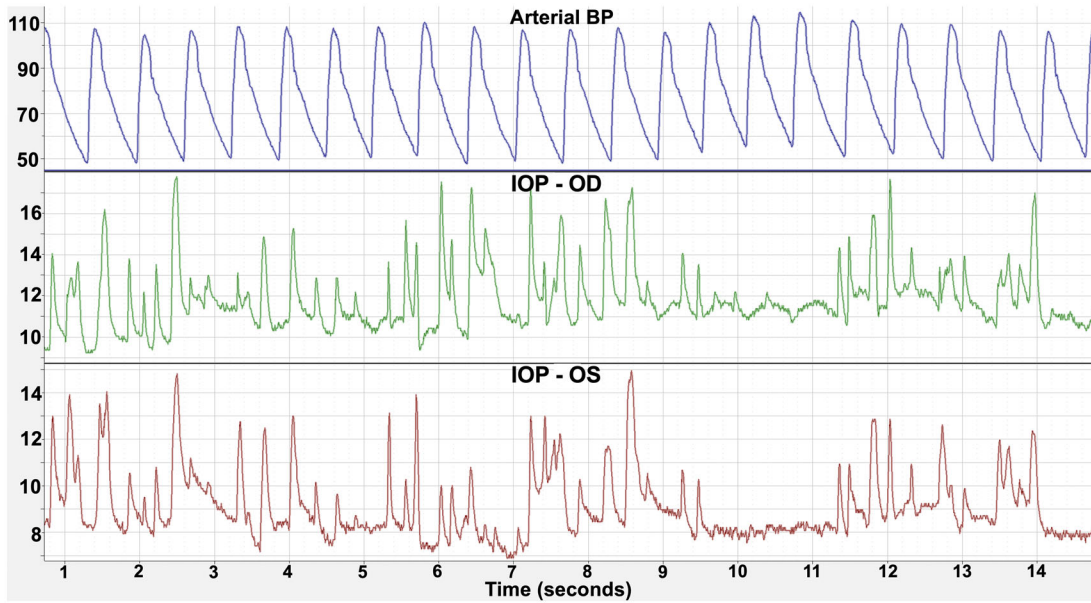


Figure 2. Screenshot of 15 seconds of pressure data (in mm Hg) in an awake, behaving NHP instrumented with the telemetry system shown in Figure 1. The magnitude and frequency of transient IOP fluctuations associated with blink and saccade are remarkably similar in fellow eyes. Note that OPA is generally obscured by the large transient IOP fluctuations when the NHPs are awake and behaving, although they are visible at time = 10 to 11.5 seconds in this tracing.

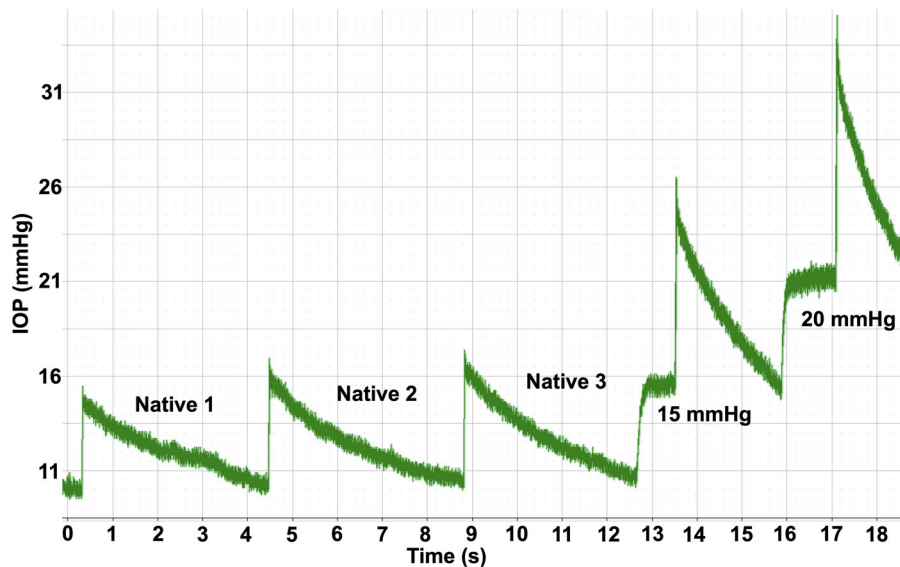


Figure 3. Screen capture of 13 minutes of IOP data measured during a typical session, with MVIs of 15 μ L administered at 5 baseline IOPs: native 1, native 2, native 3, 15 mm Hg, and 20 mm Hg.

prior to the fifth MVI. After IOP was stabilized at both the 15 and 20 mm Hg baseline IOPs, the manometer stopcock was closed immediately prior to MVI initiation to ensure that all BSS flowed into the eye and not into the manometer bottle upon injection. After each MVI, IOP was allowed to recover to within 0.5 mm Hg of the baseline IOP prior to the injection. The full set of 5 MVIs were repeated in 2 to 5 sessions at least 2 weeks

apart; the number of MVI sessions for each eye are shown in Table 1. IOP during a typical MVI is shown in Figure 3. Notably, the time of IOP recovery is much shorter with higher baseline IOPs, primarily due to greater outflow as described in Goldmann’s equation⁵⁰ as well as choroidal compression with higher IOP due to increased IOP-driven venous outflow. Additionally, viscoelastic properties also can play a role in ocular

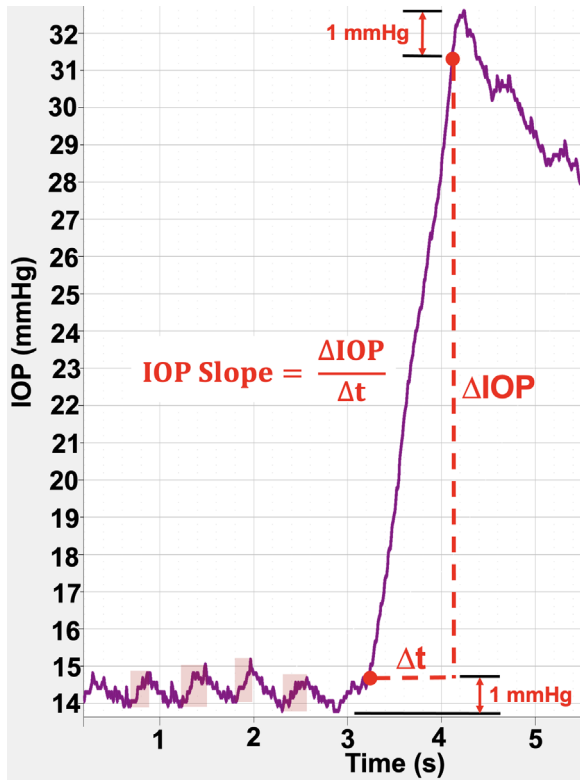


Figure 4. IOP telemetry data from a typical MVI of 15 μL at 15 mm Hg baseline IOP, showing the methodology used to calculate the change in IOP (ΔIOP) and IOP slope. The magnitude of baseline OPA (shaded red area) before the MVI was calculated as the peak minus the trough.

coat biomechanical response,⁵¹ but are likely masked by the dominant role of aqueous outflow increase after MVI.

Quantification of Parameters

For each MVI, the change in IOP (ΔIOP) was calculated as the peak of the IOP increase from the MVI minus the lowest trough, with 1 mm Hg eliminated at both the top and bottom of the upslope data to correct for IOP fluctuations resulting from OPA (Fig. 4). It is very difficult to discern the location of the start and end points of the MVI within the OPA cycle, so this scheme was implemented to reduce the confounding effects of the OPA cycle in the ΔIOP measurement. IOP slope was calculated as ΔIOP divided by the time over which IOP was rising (see Fig. 4).

Baseline OPA was calculated as the average of the five OPA cycles before the MVI (see Fig. 4). Ocular rigidity coefficients (K) were calculated according to Friedenwald's equation: $\text{IOP} = \text{IOP}_0 + \Delta\text{IOP} = \text{IOP}_0 e^{K\Delta V}$, and so $K = \frac{1}{\Delta V} \ln\left(\frac{\text{IOP}_0 + \Delta\text{IOP}}{\text{IOP}_0}\right)$, with IOP_0 representing the average baseline IOP in the 15 seconds

prior to MVI, and ΔIOP calculated to exclude OPA, as shown in Figure 4. The IOP transducer is very accurate, with a ± 0.1 mm Hg random error. We averaged OPA across five heartbeats prior to MVI to calculate baseline OPA in each session and averaged OPA data across MVI sessions within animals, which should have the effect of eliminating much of the random transducer measurement error.

Calculation of PV

The IOP slope represents the change in IOP (ΔIOP in mm Hg) over time (seconds) due to our injection volume (15 $\mu\text{L}/\text{s}$) for a given eye at a given baseline IOP, resulting in a direct experimental pressure-volume relationship for each session in each eye. The IOP slope is linear (see Figs. 3, 4) and so this relation can be used even though the change in IOP from OPA is much smaller than that from MVI. Hence, we calculated PV directly from the IOP slope, assuming that PV (μL change in volume) is directly proportional to OPA (mm Hg change in pressure) according to the following equation: $PV = \frac{15 * \text{OPA}}{\text{IOP Slope}}$, where 15 represents the experimental injection volume in μL per second.

Statistical Analysis

To avoid the possibility that differences in intra- and intersubject variability could bias our results, all parameters were averaged for each baseline IOP across all MVI sessions for each eye, resulting in one set of 5 parameters for the native 1, native 2, native 3, 15 mm Hg, and 20 mm Hg baseline IOPs for each eye. Pearson correlation coefficients were used to assess relationships between baseline OPA and ΔIOP , IOP slope, and ocular rigidity coefficients at different native baseline IOPs, with significance defined as $P \leq 0.05$. In addition, the R^2 values from linear regressions were used to assess the strength of relationships between parameters. Linear regression coefficients were used to further quantify the relationship between the baseline OPA and the ocular rigidity coefficients. A three-level nested ANOVA was used to assess the source of PV variation among eyes, among days within eyes, among trials within days within eyes, and within trials within days within eyes.

Results

Mean values and standard deviations of baseline IOP (mm Hg), ΔIOP (mm Hg), IOP slope (mm Hg/s), PV (mm Hg), baseline OPA (mm Hg), and ocular

rigidity coefficient (μL^{-1}) are shown for all NHPs in Table 2 for MVIs taken at each native baseline IOPs trial and in Table 3 for MVIs taken at an averaged native, 15 mm Hg, and 20 mm Hg baseline IOP trials. Mean parameter values and standard deviations averaged across all NHPs are shown in Table 4 for each native trial and averaged native, 15 mm Hg, and 20 mm Hg baseline IOP trials are shown in Table 5.

After MVI at native, baseline IOP of 10.4 ± 1.6 mm Hg, IOP increased by 9.1 ± 2.8 mm Hg (ΔIOP) at a 9.6 ± 2.7 mm Hg/s slope, OPA was 0.70 ± 0.13 mm Hg on average; the average ocular rigidity coefficient was $0.042 \pm 0.010 \mu\text{L}^{-1}$ and average PV was $1.16 \pm 0.43 \mu\text{L}$. At 15 mm Hg baseline IOP, the IOP increased by 12.9 ± 3.7 mm Hg (ΔIOP) at a 12.9 ± 2.6 mm Hg/s slope, OPA was 0.77 ± 0.12 mm Hg on average; the

average ocular rigidity coefficient was 0.041 ± 0.008 . At 20 mm Hg baseline IOP, the IOP increased by 15.0 ± 2.6 mm Hg (ΔIOP) at a 15.6 ± 2.8 mm Hg/s slope, OPA was 0.86 ± 0.14 mm Hg on average; the average ocular rigidity coefficient was 0.037 ± 0.005 . In general, as the baseline IOP increased, ΔIOP , IOP slope, and baseline OPA increased. The ocular rigidity coefficients exhibited a less consistent relationship with higher baseline IOPs. The average native IOP values were 10.0 ± 1.9 mm Hg at native 1, 10.5 ± 1.4 mm Hg at native 2, and 10.8 ± 1.3 mm Hg at native 3, as shown in Table 4.

The Pearson correlation coefficients for relationships between all parameters are shown in Table 6. Baseline OPA and ΔIOP , IOP slope, and ocular rigidity coefficients were also positively correlated and significant across most baseline IOPs. Linear

Table 2. Mean Baseline IOP (mm Hg), ΔIOP (mm Hg), IOP Slope (mm Hg/s), PV (μL), Baseline OPA (mm Hg), and Ocular Rigidity Coefficient (μL^{-1}) Values With Standard Deviations for Each NHP at Native Baseline IOPs

NHP - Eye Parameter/trial	13.171 - OD				13.86 - OD			
	Native 1	Native 2	Native 3	Average	Native 1	Native 2	Native 3	Average
Baseline IOP (mm Hg)	10.0 ± 0.8	10.6 ± 0.8	11.1 ± 0.8	10.6 ± 0.8	11.6 ± 1.0	11.7 ± 0.8	11.7 ± 0.7	11.7 ± 0.7
ΔIOP (mm Hg)	9.8 ± 1.0	10.6 ± 0.9	11.1 ± 1.4	10.5 ± 1.1	5.0 ± 1.7	5.6 ± 1.5	5.6 ± 1.0	5.4 ± 1.3
IOP slope (mm Hg/s)	10.5 ± 0.9	10.9 ± 1.0	11.7 ± 1.3	11.0 ± 1.1	5.5 ± 1.5	5.6 ± 1.5	6.0 ± 1.2	5.7 ± 1.2
PV (μL)	1.01 ± 0.25	0.88 ± 0.27	1.02 ± 0.21	0.97 ± 0.25	1.81 ± 0.78	1.73 ± 0.57	1.53 ± 0.53	1.69 ± 0.63
Baseline OPA (mm Hg)	0.71 ± 0.05	0.64 ± 0.11	0.79 ± 0.07	0.71 ± 0.10	0.61 ± 0.10	0.61 ± 0.04	0.59 ± 0.08	0.60 ± 0.07
Ocular rigidity coefficient (μL^{-1})	0.045 ± 0.002	0.046 ± 0.001	0.046 ± 0.002	0.046 ± 0.002	0.024 ± 0.005	0.026 ± 0.005	0.026 ± 0.003	0.025 ± 0.004
NHP - Eye Parameter/trial	150069 - OD				150110 - OD			
	Native 1	Native 2	Native 3	Average	Native 1	Native 2	Native 3	Average
Baseline IOP (mm Hg)	10.9 ± 0.1	11.1 ± 0.1	10.9 ± 0.8	11.0 ± 0.4	10.5 ± 1.9	10.8 ± 1.7	10.9 ± 1.5	10.8 ± 1.6
ΔIOP (mm Hg)	7.1 ± 0.5	7.8 ± 0.5	8.3 ± 0.6	7.7 ± 0.7	10.1 ± 3.9	12.9 ± 1.4	13.3 ± 1.7	12.1 ± 2.8
IOP slope (mm Hg/s)	7.7 ± 0.0	8.3 ± 0.2	8.5 ± 0.0	8.2 ± 0.4	11.4 ± 2.5	13.1 ± 1.8	13.4 ± 1.5	12.6 ± 2.0
PV (μL)	1.17 ± 0.21	0.95 ± 0.27	1.00 ± 0.21	1.04 ± 0.24	1.01 ± 0.26	0.87 ± 0.23	0.89 ± 0.22	0.92 ± 0.24
Baseline OPA (mm Hg)	0.60 ± 0.02	0.52 ± 0.13	0.57 ± 0.13	0.56 ± 0.09	0.74 ± 0.08	0.75 ± 0.12	0.79 ± 0.10	0.76 ± 0.09
Ocular rigidity coefficient (μL^{-1})	0.034 ± 0.002	0.036 ± 0.002	0.038 ± 0.004	0.036 ± 0.003	0.044 ± 0.011	0.053 ± 0.005	0.053 ± 0.006	0.050 ± 0.009
NHP - Eye Parameter/trial	150152 - OD				150171 - OD			
	Native 1	Native 2	Native 3	Average	Native 1	Native 2	Native 3	Average
Baseline IOP (mm Hg)	9.1 ± 0.8	9.8 ± 0.9	10.2 ± 1.1	9.7 ± 1.0	10.0 ± 2.8	10.3 ± 2.6	10.6 ± 2.4	10.3 ± 2.4
ΔIOP (mm Hg)	8.2 ± 1.7	9.9 ± 0.9	11.1 ± 1.1	9.7 ± 1.7	8.4 ± 1.6	9.4 ± 1.3	9.5 ± 1.0	9.1 ± 1.3
IOP slope (mm Hg/s)	9.0 ± 1.3	10.6 ± 1.7	11.7 ± 1.4	10.4 ± 1.7	9.0 ± 1.9	9.6 ± 1.3	10.0 ± 0.9	9.5 ± 1.4
PV (μL)	1.19 ± 0.32	1.12 ± 0.38	1.02 ± 0.22	1.11 ± 0.32	1.31 ± 0.42	1.17 ± 0.25	1.07 ± 0.22	1.18 ± 0.32
Baseline OPA (mm Hg)	0.72 ± 0.23	0.81 ± 0.27	0.79 ± 0.12	0.77 ± 0.20	0.75 ± 0.04	0.73 ± 0.05	0.71 ± 0.05	0.73 ± 0.04
Ocular rigidity coefficient (μL^{-1})	0.043 ± 0.005	0.047 ± 0.004	0.049 ± 0.003	0.046 ± 0.005	0.041 ± 0.004	0.044 ± 0.005	0.043 ± 0.004	0.043 ± 0.004
NHP - Eye Parameter/trial	150172 - OS							
	Native 1	Native 2	Native 3	Average				
Baseline IOP (mm Hg)	8.0 ± 2.6	9.7 ± 0.5	10 ± 0.5	9.3 ± 1.6				
ΔIOP (mm Hg)	6.1 ± 1.9	6.4 ± 0.8	6.8 ± 0.9	6.4 ± 1.2				
IOP slope (mm Hg/s)	6.4 ± 1.8	6.7 ± 0.5	7.3 ± 0.8	6.8 ± 1.1				
PV (μL)	1.45 ± 0.43	1.39 ± 0.39	1.16 ± 0.30	1.33 ± 0.39				
Baseline OPA (mm Hg)	0.61 ± 0.14	0.62 ± 0.10	0.56 ± 0.11	0.60 ± 0.10				
Ocular rigidity coefficient (μL^{-1})	0.041 ± 0.021	0.034 ± 0.004	0.034 ± 0.004	0.036 ± 0.011				

Table 3. Mean Baseline IOP (mm Hg), ΔIOP (mm Hg), IOP Slope (mm Hg/s), PV (μL), Baseline OPA (mm Hg), and Ocular Rigidity Coefficient (μL⁻¹) Values With Standard Deviations for Each NHP at Averaged Native, 15 mm Hg, and 20 mm Hg Baseline IOPs

NHP - Eye Parameter/Baseline IOP	13.171 - OD			13.86 - OD		
	Native	15 mm Hg	20 mm Hg	Native	15 mm Hg	20 mm Hg
ΔIOP (mm Hg)	10.5 ± 1.1	13.4 ± 0.4	16.1 ± 2.3	5.4 ± 1.3	8.2 ± 0.5	10.3 ± 0.2
IOP slope (mm Hg/s)	11.0 ± 1.1	14.0 ± 0.7	16.7 ± 1.8	5.7 ± 1.2	8.7 ± 1.0	10.9 ± 0.4
ΔOPA (mm Hg)	0.14 ± 0.14	0.34 ± 0.14	0.39 ± 0.12	0.05 ± 0.05	0.16 ± 0.06	0.15 ± 0.06
Baseline OPA (mm Hg)	0.71 ± 0.10	0.71 ± 0.20	0.73 ± 0.05	0.60 ± 0.07	0.65 ± 0.04	0.71 ± 0.03
Ocular rigidity coefficient (μL⁻¹)	0.046 ± 0.002	0.042 ± 0.001	0.039 ± 0.004	0.025 ± 0.004	0.029 ± 0.001	0.028 ± 0.001
150069 - OD						
150110 - OD						
NHP - Eye Parameter/Baseline IOP	Native	15 mm Hg	20 mm Hg	Native	15 mm Hg	20 mm Hg
ΔIOP (mm Hg)	7.7 ± 0.7	10.4 ± 0.2	12.8 ± 0.1	12.1 ± 2.8	17.3 ± 5.3	17.3 ± 1.5
IOP slope (mm Hg/s)	8.2 ± 0.4	10.8 ± 0.5	13.1 ± 1.3	12.6 ± 2.0	14.7 ± 2.5	18.0 ± 2.1
ΔOPA (mm Hg)	0.17 ± 0.08	0.16 ± 0.01	0.17 ± 0.14	0.27 ± 0.17	0.31 ± 0.08	0.31 ± 0.11
Baseline OPA (mm Hg)	0.56 ± 0.09	0.65 ± 0.02	0.72 ± 0.05	0.76 ± 0.09	0.86 ± 0.09	0.97 ± 0.15
Ocular rigidity coefficient (μL⁻¹)	0.036 ± 0.003	0.035 ± 0.001	0.033 ± 0.000	0.050 ± 0.009	0.050 ± 0.010	0.041 ± 0.003
150152 - OD						
150171 - OD						
NHP - Eye Parameter/Baseline IOP	Native	15 mm Hg	20 mm Hg	Native	15 mm Hg	20 mm Hg
ΔIOP (mm Hg)	9.7 ± 1.7	14.0 ± 1.1	16.5 ± 1.3	9.1 ± 1.3	12.7 ± 1.6	15.6 ± 2.0
IOP slope (mm Hg/s)	10.4 ± 1.7	15.4 ± 1.2	17.8 ± 1.2	9.5 ± 1.4	12.8 ± 1.6	15.7 ± 1.2
ΔOPA (mm Hg)	0.21 ± 0.13	0.26 ± 0.19	0.27 ± 0.08	0.14 ± 0.11	0.18 ± 0.16	0.14 ± 0.29
Baseline OPA (mm Hg)	0.77 ± 0.20	0.83 ± 0.09	0.88 ± 0.10	0.73 ± 0.04	0.76 ± 0.07	0.92 ± 0.09
Ocular rigidity coefficient (μL⁻¹)	0.046 ± 0.005	0.044 ± 0.002	0.040 ± 0.002	0.043 ± 0.004	0.041 ± 0.004	0.038 ± 0.004
150172 - OS						
NHP - Eye Parameter/Baseline IOP	Native	15 mm Hg	20 mm Hg			
ΔIOP (mm Hg)	6.4 ± 1.2	10.3 ± 0.2	13.3 ± 0.1			
IOP slope (mm Hg/s)	6.8 ± 1.1	11.2 ± 0.5	13.5 ± 0.6			
ΔOPA (mm Hg)	0.20 ± 0.05	0.31 ± 0.05	0.22 ± 0.03			
Baseline OPA (mm Hg)	0.60 ± 0.10	0.76 ± 0.07	0.97 ± 0.11			
Ocular rigidity coefficient (μL⁻¹)	0.036 ± 0.011	0.035 ± 0.001	0.034 ± 0.000			

Table 4. Mean Baseline IOP (mm Hg), ΔIOP (mm Hg), IOP Slope (mm Hg/s), PV (μL), Baseline OPA (mm Hg), and Ocular Rigidity Coefficient (μL⁻¹) Values With Standard Deviations Across all NHPs, for MVIs Performed at Native Baseline IOPs

Average Parameter/Trial	Native 1	Native 2	Native 3	Average
Baseline IOP (mm Hg)	10.0 ± 1.9	10.5 ± 1.4	10.8 ± 1.3	10.4 ± 1.6
ΔIOP (mm Hg)	8.1 ± 2.7	9.4 ± 2.7	9.8 ± 2.8	9.1 ± 2.8
IOP slope (mm Hg/s)	8.8 ± 2.6	9.7 ± 2.8	10.2 ± 2.8	9.6 ± 2.7
PV (μL)	1.26 ± 0.48	1.14 ± 0.44	1.08 ± 0.33	1.16 ± 0.43
Baseline OPA (mm Hg)	0.69 ± 0.12	0.69 ± 0.15	0.71 ± 0.13	0.70 ± 0.13
Ocular rigidity coefficient (μL⁻¹)	0.040 ± 0.011	0.042 ± 0.010	0.043 ± 0.010	0.042 ± 0.010

regression R² values for all parameter comparisons are shown in Table 6, and the regression goodness of fit mirrors the results for the Pearson correlations.

Graphical representations of the linear regression relationships between baseline OPA and ocular rigid-

ity coefficients are found in Figure 5, and the associated regression coefficients are shown in Table 7. Regression coefficients were moderately large, showing that even small increases in OPA predicted fairly large changes in the ocular rigidity coefficient. The R² values indicate that 50% of the variability in the ocular rigidity coeffi-

Table 5. Mean Δ IOP (mm Hg), IOP Slope (mm Hg/s), Δ OPA (mm Hg), and Baseline OPA (mm Hg) Values With Standard Deviations Across all NHPs, for MVIs Performed at Averaged Native, 15 mm Hg, and 20 mm Hg Baseline IOPs

Average Parameter/Baseline IOP	Native	15 mm Hg	20 mm Hg
ΔIOP (mm Hg)	9.1 \pm 2.8	12.9 \pm 3.7	15.0 \pm 2.6
IOP slope (mm Hg/s)	9.6 \pm 2.7	12.9 \pm 2.6	15.6 \pm 2.8
Baseline OPA (mm Hg)	0.70 \pm 0.13	0.77 \pm 0.12	0.86 \pm 0.14
Ocular rigidity coefficient (μL^{-1})	0.042 \pm 0.010	0.041 \pm 0.008	0.037 \pm 0.005

Table 6. Pearson Correlation Coefficients and Linear Regression R² Values Comparing Parameters From Successive MVIs Taken at Native Baseline IOP (3 Trials) and Both 15 mm Hg and 20 mm Hg Baseline IOPs, With Significance Defined as * $P \leq 0.05$ and ** $P < 0.01$

Trial Parameter Comparison/Statistic	Native 1		Native 2		Native 3		15 mm Hg		20 mm Hg	
	Pearson	R2	Pearson	R2	Pearson	R2	Pearson	R2	Pearson	R2
Baseline OPA (mm Hg) versus ΔIOP (mm Hg)	0.828**	0.686*	0.610	0.373	0.897**	0.805**	0.845**	0.714*	0.521	0.272
Baseline OPA (mm Hg) versus IOP slope (mm Hg/s)	0.822**	0.676*	0.622	0.387	0.918**	0.843**	0.810**	0.656*	0.477	0.228
Baseline OPA (mm Hg) versus ocular rigidity coefficient (μL^{-1})	0.708*	0.501	0.695*	0.483	0.871*	0.759**	0.840**	0.705*	0.527	0.278

lients during the initial trial (native 1) can be explained by differences in OPA measured at native IOP, as shown in Table 6.

Table 7. Regression Coefficients, Intercept Values, and P Values for Baseline OPA as a Predictor of Ocular Rigidity Coefficient

Trial	Slope	Intercept	P Value
Native 1	0.078	-0.014	0.075
Native 2	0.065	-0.003	0.083
Native 3	0.075	-0.010	0.011
15 mm Hg	0.072	-0.014	0.018
20 mm Hg	0.022	0.018	0.223

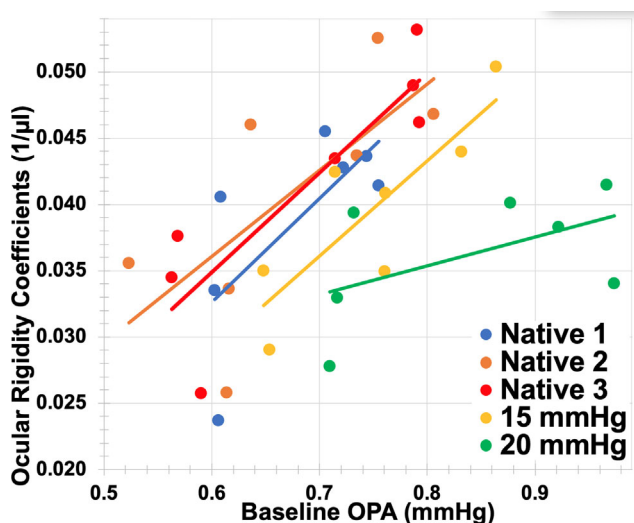


Figure 5. Scatter plots and linear regression lines showing the relationships between baseline OPA (mm Hg) and the ocular rigidity coefficients (μL^{-1}) at native 1 (dark blue circles), native 2 (orange circles), native 3 (red circles), 15 mm Hg (yellow circles), and 20 mm Hg (green circles) baseline IOPs. The gray line is the average linear fit of all native IOP data.

From Table 8, the PV was significantly different between trials within days within eyes, between days within eyes, and between eyes.

Discussion

Ocular coat mechanical behavior can be accurately assessed using controlled MVIs as an ocular volume-pressure test in the living eye. Strong, significant correlations (high Pearson correlation coefficients and $P \leq 0.05$) were observed between baseline OPA and Δ IOP, IOP slope, and ocular rigidity coefficients. Strong positive correlations among these parameters

Table 8. Three-Level Nested ANOVA Analyzing Source of Variation of PV (μL) Among Eyes, Among Days Within Eyes, Among Trials Within Days Within Eyes, and Within Trials Within Days Within Eyes Among Native IOP Trials

Source of Variation/Statistic	SS	df	MS	F	P Value
Among eyes	20.35	6	3.39	3.25	0.026
Among days within eyes	17.74	17	1.04	8.46	<0.001
Among trials within days within eyes	5.92	48	0.12	1.66	0.007
Within trials within days within eyes	21.41	288	0.07		
Total	65.42	359			

indicate tight coupling of the various aspects of the ocular coat mechanical response. Most importantly, OPA at native IOP, which can be measured noninvasively in the clinic, is correlated to ocular rigidity, a useful parameter for which there is currently no widely accepted noninvasive clinical measure.

Prior studies reported a significant positive relationship between OPA and the ocular rigidity coefficient in human patients at manometrically controlled IOPs, although no results were reported at native resting IOP.³⁴ We verified these relationships in primates at manometrically controlled baseline IOPs of 15 mm Hg and 20 mm Hg using indwelling IOP telemetry transducers. In the present study, a significant positive relationship between OPA and the ocular rigidity coefficient also held at native baseline IOPs, as well as at 15 mm Hg baseline IOP shown in prior work, suggesting that OPA at resting IOP can be used as a biomarker of ocular rigidity in individual eyes, without estimation of the OPA-related change in ocular volume. Prior studies reported a weak, yet significant association with OPA and ocular rigidity using noninvasive clinical estimations of ocular rigidity,^{39,41,42} but we observed much larger R^2 values when comparing OPA and ocular rigidity coefficients at native IOPs in this study, likely due to the error inherent in noninvasive ocular rigidity estimation.⁴¹ Additionally, these relationships were also present with other measures of ocular coat mechanical behavior, including ΔIOP and IOP slope. Strong relationships were present among the three different measures of ocular coat mechanical response associated with MVI, namely ΔIOP , IOP slope, and ocular rigidity coefficient, as expected. The lack of a perfect, one-to-one relationship between ΔIOP and IOP slope measured with MVI and ocular rigidity coefficients at native IOP could be because the IOP measured during each MVI is confounded with OPA due to cardiac cycles occurring during the course of the injection. This resulted in portions of OPA (both the IOP elevation and change in ocular blood volume) being included in the parameter calculations. To compensate for this, 1 mm Hg of the rise in IOP at both the beginning and

end of the MVI-driven IOP elevation was excluded for the purposes of calculating the ΔIOP reported and included in the calculation of the ocular rigidity coefficient. The mean ocular rigidity coefficients of $0.042 \mu\text{L}^{-1}$ reported herein for native baseline IOPs in NHPs (see Table 3) agree extremely well with previous reports ($0.0412 \mu\text{L}^{-1}$).^{33,52} This value is much larger than the $0.0235 \mu\text{L}^{-1}$ reported for humans,³³ which is somewhat counterintuitive because the sclera is much thinner in NHPs compared to humans.^{48,53,54} From these data, we can conclude that NHPs exhibit a higher rate of ocular coat stiffening for a given ocular volume change compared to humans. It is also possible that the NHP ocular coat is materially stiffer than that of humans such that the overall structural stiffness of the NHP ocular coat is higher than that of humans despite being thinner, although prior reports have not quantified this material property difference using approaches that are similar enough to allow for direct comparison.^{55–59}

Friedenwald's equation is: $\text{IOP} = \text{IOP}_0 + \Delta\text{IOP} = \text{IOP}_0 e^{K\Delta V}$, where K is the ocular rigidity coefficient, IOP_0 is the baseline IOP, ΔIOP is the IOP change, and ΔV is the ocular volume change. From this equation, we can calculate ocular rigidity coefficient as $K = \frac{1}{\Delta V} \ln\left(\frac{\text{IOP}_0 + \Delta\text{IOP}}{\text{IOP}_0}\right)$. The exponential relationship inherent in Friedenwald's equation accounts for corneoscleral hyperelasticity, because ΔIOP is larger at larger baseline IOPs (IOP_0). Friedenwald's equation is an approximation based on experimental observations; if the relationship between IOP_0 and ΔIOP with constant values of ΔV is not exactly exponential with the natural log, then ocular rigidity coefficient (K) can change with IOP_0 . In this case, ocular rigidity coefficient decreases with increasing baseline IOPs (IOP_0), and this change is especially large at 20 mm Hg baseline IOP. We also observe insignificant and weaker R^2 values and Pearson correlation coefficients at 20 mm Hg baseline IOP. These results indicate that the corneoscleral shell of Rhesus macaques does not stiffen in a perfectly exponential manner with increases in IOP (i.e. the shape of the curve changes slightly with increasing baseline IOP). This suggests that the

exponential functional form is not an exact fit for the hyperelastic stiffening of the corneoscleral shell in Rhesus macaques, especially at higher baseline IOPs, which could be due to any number of factors.

Prior studies have suggested that OPA is larger at higher baseline IOPs^{34,60} and that ocular coats are stiffer at higher IOPs.^{33,34,52,55,59} Prior studies have also shown that ocular blood flow autoregulation ensures that blood injection volume remains relatively consistent as IOP increases within the limits of IOP used in our experiments.^{35–38} The moderate relationship between baseline OPA and Δ OPA suggests that initial OPA has some utility in predicting the eye-specific increase in OPA that occurs with IOP elevation (a measure of ocular coat hyperelastic stiffening), but it is not as important as the ocular rigidity coefficient. The significant positive relationship between OPA and the ocular rigidity coefficient observed at manometrically controlled baseline IOPs of 15 and 20 mm Hg agree with results reported previously in human patients, reinforcing the notion that the NHP is a good model of human ocular coat mechanical behavior. Further, this relationship holds at native baseline IOP, agreeing with prior reports.^{39,42} This particular result suggests that OPA measured in the clinic without IOP control is significantly correlated with ocular rigidity, and therefore OPA at native IOP can serve as a biomarker ocular coat mechanical behavior.

Prior studies have found that PV estimated from OCT images of choroidal volume change with cardiac cycle in humans to be $7.8 \pm 4.9 \mu\text{L}$ ³⁹ and using AC manometry in humans at 15 mm Hg to be $6.03 \pm 1.32 \mu\text{L}$.³⁴ We would expect PV in our study to be roughly approximately 70% of these values given that the NHP globe is roughly approximately 70% of the human globe, based solely on relative eye volume and the similarity of their visual systems. That said, differences in ocular coat mechanical behavior (ocular rigidity) and baseline IOP could significantly affect these comparisons. The average PV of $1.16 \pm 0.43 \mu\text{L}$ in NHPs, which has not been previously reported to our knowledge, suggest that PV in humans and NHPs is not comparable as expected. One explanation for this finding could be the difference in OPA reported for humans and NHPs: prior studies have reported human OPA to be $2.2 \pm 0.6 \text{ mm Hg}$ at baseline IOPs under 22 mm Hg using a Pascal dynamic contour tonometer (DCT),⁶¹ whereas we observed OPAs of $0.70 \pm 0.13 \text{ mm Hg}$ at native baseline IOP, $0.77 \pm 0.12 \text{ mm Hg}$ at 15 mm Hg baseline IOP, and $0.86 \pm 0.14 \text{ mm Hg}$ at 20 mm Hg baseline. Coupled with the fact that the ocular rigidity coefficient is larger in NHPs than humans, these data suggest that PV is much smaller in NHPs as reported herein. Although PV could be calculated from OPA and the ocular rigid-

ity coefficient (K), it should be noted that Friedenwald's equation to determine K is an imperfect fit to experimental data. Our eye-specific calculations of PV reported herein are based on precise experimental measures obtained under tightly controlled conditions, and so are likely to be more accurate as a result.

This study is limited by the following considerations. First, this study uses NHPs as a model for human ocular behavior, and the reported results may not translate into patients given their inherent differences in ocular mechanical response. However, NHPs develop experimental glaucoma that is similar to the human disease and have the most similar ocular coat mechanics and anatomy of all animal models.^{45,46} Second, we had a limited sample size (7 eyes in 7 animals) whose ocular biomechanical response after MVI may not be representative of the greater population. In spite of this, we found statistically significant relationships between the reported parameters along with a large effect size, and therefore a larger cohort would likely confirm the reported results. Third, MVI sessions were not conducted at the same time of day, although this is unlikely to affect our results or conclusions because MVI is an acute test using relative IOP change that should not be affected by variations in native IOP and other variables that exhibit diurnal variation. In addition, natural diurnal IOP variation is accommodated in the error term of our statistical analyses, and so this is actually a strength of the study. Finally, we assumed that aqueous humor outflow did not decrease the volume of the eye during the 1-second injection. The statistical relationship between ocular rigidity and OPA is not as strong at a baseline IOP of 20 mm Hg compared with native and 15 mm Hg baseline IOPs; we believe this to be due to the lower systemic blood pressure in NHPs under isoflurane anesthesia, resulting in lower and more variable OPA at 20 mm Hg baseline IOPs. In this scenario, this finding is not a reflection of the ocular rigidity-to-OPA relationship that would be present in a non-anesthetized NHP or a human patient at 20 mm Hg IOP with normal blood pressures, although this should be confirmed in future studies. Our data suggest that IOP does not decrease significantly due to aqueous outflow on the 1-second injection timescale. If one considers the post-MVI IOP decay seen in the figures, it is apparent that IOP decreases 2 to 3 mm Hg/second immediately following MVI. This occurs when IOP is at its peak value, however, and so it is unclear how much aqueous outflow would occur during the 1-second injection, as IOP is rapidly increasing during the injection time course and outflow is highest only when IOP is highest. So, estimating ocular rigidity assuming no outflow occurs during the injection as

well as is a reasonable approach. It is also reasonable to assume that ocular coat stiffness far outweighs aqueous outflow effects in the calculation of the ocular rigidity coefficient. To calculate the IOP rise due to MVI (Δ IOP), we added 1 mm Hg to the minimum IOP and subtracted 1 mm Hg from the maximum IOP values to account for the variable contributions of OPA that occur during MVI. This assumption, along with the assumptions that ocular coat viscoelastic effects and choroidal volume changes are minimal over the 1 second time course of MVI, likely add some error to the measurements reported herein. In spite of these assumptions, our ocular rigidity coefficient estimates closely match those of prior reports for Rhesus macaques from Friedenwald and Clarke,^{33,52} and the R^2 values reported herein between ocular rigidity and OPA are stronger than those reported previously.^{39,41}

In summary, significant positive relationships were found between ocular rigidity and OPA using continuous IOP telemetry and MVIs in NHPs. Ocular pulse volume in NHPs is much lower than in humans, even when compensating for differences in eye volume. Most importantly, OPA at native IOP predicts ocular rigidity despite variability in PV between cardiac cycles and therefore clinically measured OPA may serve as a biomarker of ocular coat biomechanical behavior.

Acknowledgments

The authors thank Lisa Hethcox, LVT, and Candice Jackson, LVT, for their invaluable assistance in the oversight and management of the NHPs and in data collection, as well as Chester Calvert for his invaluable assistance in the acquisition, filtering, and processing of data.

Supported by NIH Grants R01-EY026035, and P30-EY003039; EyeSight Foundation of Alabama (unrestricted departmental funds); Research to Prevent Blindness (unrestricted departmental funds).

Disclosure: **J.E. Marker**, None; **D.C. Turner**, None; **J.V. Jasien**, None; **C.N.A. Nyankerh**, None; **B.C. Samuels**, None; **J.C. Downs**, None

References

1. Quigley H, Anderson DR. The dynamics and location of axonal transport blockade by acute intraocular pressure elevation in primate optic nerve. *Invest Ophthalmol*. 1976;15:606–616.
2. Howell GR, Libby RT, Jakobs TC, et al. Axons of retinal ganglion cells are insulted in the optic nerve early in DBA/2J glaucoma. *J Cell Biol*. 2007;179:1523–1537.
3. Balaratnasingam C, Morgan WH, Bass L, Match G, Cringle SJ, Yu DY. Axonal transport and cytoskeletal changes in the laminar regions after elevated intraocular pressure. *Invest Ophthalmol Vis Sci*. 2007;48:3632–3644.
4. Balaratnasingam C, Morgan WH, Bass L, et al. Elevated pressure induced astrocyte damage in the optic nerve. *Brain Res*. 2008;1244:142–154.
5. Nickells RW, Howell GR, Soto I, John SW. Under pressure: cellular and molecular responses during glaucoma, a common neurodegeneration with axonopathy. *Annu Rev Neurosci*. 2012;35:153–179.
6. Sommer A. Glaucoma risk factors observed in the Baltimore Eye Survey. *Curr Opin Ophthalmol*. 1996;7:93–98.
7. Coleman AL, Gordon MO, Beiser JA, Kass MA, Ocular Hypertension Treatment S. Baseline risk factors for the development of primary open-angle glaucoma in the Ocular Hypertension Treatment Study. *Am J Ophthalmol*. 2004;138:684–685.
8. Nouri-Mahdavi K, Hoffman D, Coleman AL, et al. Predictive factors for glaucomatous visual field progression in the Advanced Glaucoma Intervention Study. *Ophthalmology*. 2004;111:1627–1635.
9. European Glaucoma Prevention Study G, Miglior S, Pfeiffer N, et al. Predictive factors for open-angle glaucoma among patients with ocular hypertension in the European Glaucoma Prevention Study. *Ophthalmology*. 2007;114:3–9.
10. Leske MC, Heijl A, Hyman L, Bengtsson B, Dong L, Yang Z. Predictors of long-term progression in the early manifest glaucoma trial. *Ophthalmology*. 2007;114:1965–1972.
11. Leske MC, Wu SY, Hennis A, Honkanen R, Nemesure B. Risk factors for incident open-angle glaucoma: the Barbados Eye Studies. *Ophthalmology*. 2008;115:85–93.
12. Tielsch JM, Katz J, Sommer A, Quigley HA, Javitt JC. Hypertension, perfusion pressure, and primary open-angle glaucoma. A population-based assessment. *Arch Ophthalmol*. 1995;113:216–221.
13. Flammer J, Orgul S, Costa VP, et al. The impact of ocular blood flow in glaucoma. *Prog Retin Eye Res*. 2002;21:359–393.
14. Memarzadeh F, Ying-Lai M, Chung J, Azen SP, Varma R, Los Angeles Latino Eye Study G. Blood pressure, perfusion pressure, and open-angle glaucoma: the Los Angeles Latino Eye Study. *Invest Ophthalmol Vis Sci*. 2010;51:2872–2877.

15. Wax MB. Is there a role for the immune system in glaucomatous optic neuropathy? *Curr Opin Ophthalmol.* 2000;11:145–150.
16. Wax MB. The case for autoimmunity in glaucoma. *Exp Eye Res.* 2011;93:187–190.
17. Tezel G. The immune response in glaucoma: a perspective on the roles of oxidative stress. *Exp Eye Res.* 2011;93:178–186.
18. Morgan WH, Yu DY, Balaratnasingam C. The role of cerebrospinal fluid pressure in glaucoma pathophysiology: the dark side of the optic disc. *J Glaucoma.* 2008;17:408–413.
19. Berdahl JP, Allingham RR, Johnson DH. Cerebrospinal fluid pressure is decreased in primary open-angle glaucoma. *Ophthalmology.* 2008;115:763–768.
20. Jonas JB, Ritch R, Panda-Jonas S. Cerebrospinal fluid pressure in the pathogenesis of glaucoma. *Prog Brain Res.* 2015;221:33–47.
21. Hou R, Zhang Z, Yang D, et al. Pressure balance and imbalance in the optic nerve chamber: The Beijing Intracranial and Intraocular Pressure (iCOP) Study. *Sci China Life Sci.* 2016;59:495–503.
22. Kass MA, Heuer DK, Higginbotham EJ, et al. The Ocular Hypertension Treatment Study - A randomized trial determines that topical ocular hypotensive medication delays or prevents the onset of primary open-angle glaucoma. *Arch Ophthalmol - Chic.* 2002;120:701–713.
23. Musch DC, Gillespie BW, Niziol LM, Lichter PR, Varma R, Group CS. Intraocular pressure control and long-term visual field loss in the Collaborative Initial Glaucoma Treatment Study. *Ophthalmology.* 2011;118:1766–1773.
24. Musch DC, Gillespie BW, Lichter PR, Niziol LM, Janz NK, CIGTS Study Investigators. Visual field progression in the Collaborative Initial Glaucoma Treatment Study the impact of treatment and other baseline factors. *Ophthalmology.* 2009;116:200–207.
25. Coleman DJ, Trokel S. Direct-recorded intraocular pressure variations in a human subject. *Arch Ophthalmol.* 1969;82:637–640.
26. Jasien JV, Turner DC, Girkin CA, Downs JC. Cyclic Pattern of Intraocular Pressure (IOP) and Transient IOP Fluctuations in Nonhuman Primates Measured with Continuous Wireless Telemetry. *Curr Eye Res.* 2019;44(11):1244–1252.
27. Markert JE, Jasien JV, Turner DC, Huisinigh C, Girkin CA, Downs JC. IOP, IOP Transient Impulse, Ocular Perfusion Pressure, and Mean Arterial Pressure Relationships in Nonhuman Primates Instrumented With Telemetry. *Invest Ophthalmol Vis Sci.* 2018;59:4496–4505.
28. Turner DC, Edmiston AM, Zohner YE, et al. Transient Intraocular Pressure Fluctuations: Source, Magnitude, Frequency, and Associated Mechanical Energy. *Invest Ophthalmol Vis Sci.* 2019;60:2572–2582.
29. Liu J, He X. Corneal stiffness affects IOP elevation during rapid volume change in the eye. *Invest Ophthalmol Vis Sci.* 2009;50:2224–2229.
30. Clayson K, Pan X, Pavlatos E, et al. Corneoscleral stiffening increases IOP spike magnitudes during rapid microvolumetric change in the eye. *Exp Eye Res.* 2017;165:29–34.
31. Morris HJ, Tang J, Cruz Perez B, et al. Correlation between biomechanical responses of posterior sclera and IOP elevations during micro intraocular volume change. *Invest Ophthalmol Vis Sci.* 2013;54:7215–7222.
32. Downs JC. IOP telemetry in the nonhuman primate. *Exp Eye Res.* 2015;141:91–98.
33. Friedenwald JS. Contribution to the Theory and Practice of Tonometry. *Am J Ophthalmol.* 1937;20:985–1024.
34. Dastiridou AI, Ginis HS, De Brouwere D, Tsilimbaris MK, Pallikaris IG. Ocular rigidity, ocular pulse amplitude, and pulsatile ocular blood flow: the effect of intraocular pressure. *Invest Ophthalmol Vis Sci.* 2009;50:5718–5722.
35. Geijer C, Bill A. Effects of raised intraocular pressure on retinal, prelaminar, laminar, and retrolaminar optic nerve blood flow in monkeys. *Invest Ophthalmol Vis Sci.* 1979;18:1030–1042.
36. Kiel JW, Shepherd AP. Autoregulation of choroidal blood flow in the rabbit. *Invest Ophthalmol Vis Sci.* 1992;33:2399–2410.
37. Wang L, Burgoyne CF, Cull G, Thompson S, Fortune B. Static blood flow autoregulation in the optic nerve head in normal and experimental glaucoma. *Invest Ophthalmol Vis Sci.* 2014;55:873–880.
38. Wang L, Cull GA, Piper C, Burgoyne CF, Fortune B. Anterior and posterior optic nerve head blood flow in nonhuman primate experimental glaucoma model measured by laser speckle imaging technique and microsphere method. *Invest Ophthalmol Vis Sci.* 2012;53:8303–8309.
39. Beaton L, Mazzaferri J, Lalonde F, et al. Non-invasive measurement of choroidal volume change and ocular rigidity through automated segmentation of high-speed OCT imaging. *Biomed Opt Express.* 2015;6:1694–1706.
40. Pallikaris IG, Kymionis GD, Ginis HS, Kounis GA, Tsilimbaris MK. Ocular rigidity in living human eyes. *Invest Ophthalmol Vis Sci.* 2005;46:409–414.

41. Sayah DN, Mazzaferri J, Ghesquiere P, et al. Non-invasive in vivo measurement of ocular rigidity: Clinical validation, repeatability and method improvement. *Exp Eye Res.* 2020;190:107831.
42. Ma Y, Moroi SE, Roberts CJ. Non-invasive Clinical Measurement of Ocular Rigidity and Comparison to Biomechanical and Morphological Parameters in Glaucomatous and Healthy Subjects. *Front Med (Lausanne).* 2021;8:701997.
43. Sherwood JM, Boazak EM, Feola AJ, Parker K, Ethier CR, Overby DR. Measurement of Ocular Compliance Using iPerfusion. *Front Bioeng Biotechnol.* 2019;7:276.
44. Downs JC, Burgoyne CF, Seigfreid WP, Reynaud JF, Strouthidis NG, Sallee V. 24-hour IOP telemetry in the nonhuman primate: implant system performance and initial characterization of IOP at multiple timescales. *Invest Ophthalmol Vis Sci.* 2011;52:7365–7375.
45. Quigley HA, Dorman-Pease ME, Brown AE. Quantitative study of collagen and elastin of the optic nerve head and sclera in human and experimental monkey glaucoma. *Curr Eye Res.* 1991;10:877–888.
46. Burgoyne CF. The non-human primate experimental glaucoma model. *Exp Eye Res.* 2015;141:57–73.
47. Jasien JV, Samuels BC, Johnston JM, Downs JC. Diurnal Cycle of Translaminar Pressure in Nonhuman Primates Quantified with Continuous Wireless Telemetry. *Invest Ophthalmol Vis Sci.* 2020;61(2):37.
48. Downs JC, Blidner RA, Bellezza AJ, Thompson HW, Hart RT, Burgoyne CF. Peripapillary scleral thickness in perfusion-fixed normal monkey eyes. *Invest Ophthalmol Vis Sci.* 2002;43:2229–2235.
49. Jasien JV, Girkin CA, Downs JC. Effect of Anesthesia on Intraocular Pressure Measured With Continuous Wireless Telemetry in Nonhuman Primates. *Invest Ophthalmol Vis Sci.* 2019;60:3830–3834.
50. Goel M, Picciani RG, Lee RK, Bhattacharya SK. Aqueous humor dynamics: a review. *Open Ophthalmol J.* 2010;4:52–59.
51. Downs JC, Suh JK, Thomas KA, Bellezza AJ, Hart RT, Burgoyne CF. Viscoelastic material properties of the peripapillary sclera in normal and early-glaucoma monkey eyes. *Invest Ophthalmol Vis Sci.* 2005;46:540–546.
52. Clark JH. A Method for Measuring Elasticity In Vivo and Results Obtained on the Eyeball at Different Intraocular Pressures. *Am J Physiol.* 1932;101:474–481.
53. Downs JC, Ensor ME, Bellezza AJ, Thompson HW, Hart RT, Burgoyne CF. Posterior scleral thickness in perfusion-fixed normal and early-glaucoma monkey eyes. *Invest Ophthalmol Vis Sci.* 2001;42:3202–3208.
54. Norman RE, Flanagan JG, Rausch SM, et al. Dimensions of the human sclera: Thickness measurement and regional changes with axial length. *Exp Eye Res.* 2010;90:277–284.
55. Girard MJ, Suh JK, Bottlang M, Burgoyne CF, Downs JC. Scleral biomechanics in the aging monkey eye. *Invest Ophthalmol Vis Sci.* 2009;50:5226–5237.
56. Girard MJ, Suh JK, Bottlang M, Burgoyne CF, Downs JC. Biomechanical changes in the sclera of monkey eyes exposed to chronic IOP elevations. *Invest Ophthalmol Vis Sci.* 2011;52:5656–5669.
57. Eilaghi A, Flanagan JG, Brodland GW, Ethier CR. Strain uniformity in biaxial specimens is highly sensitive to attachment details. *J Biomechanic Engineering.* 2009;131:091003.
58. Geraghty B, Jones SW, Rama P, Akhtar R, Elsheikh A. Age-related variations in the biomechanical properties of human sclera. *J Mech Behav Biomed Mater.* 2012;16:181–191.
59. Grytz R, Fazio MA, Girard MJ, et al. Material properties of the posterior human sclera. *J Mech Behav Biomed Mater.* 2014;29:602–617.
60. Downs JC. Optic nerve head biomechanics in aging and disease. *Exp Eye Res.* 2015;133:19–29.
61. Pourjavan S, Boelle PY, Detry-Morel M, De Potter P. Physiological diurnal variability and characteristics of the ocular pulse amplitude (OPA) with the dynamic contour tonometer (DCT-Pascal). *Intl Ophthalmol.* 2007;27:357–360.